A Comparative Study of Gamma Radiation Effects on Ultra-Low Input Bias Current Linear Circuits Under Biased Conditions

Vivek Agarwal, V. P. Sundarsingh, and V. Ramachandran

***Abstract*—Ultra-low input bias current linear circuits are used in several applications requiring them to work under varying conditions of temperature, humidity, radiation etc. which influence their performance. This paper presents a first time study of gamma radiation effects on ultra low input bias current linear circuits under biased conditions for small signal dc applications. Under biased conditions, radiation-induced photo currents play a significant role. A noncatastrophic radiation leakage environment has been considered. The linear circuits selected are of different makes and have different input stages, such as those based on JFET and MOS structures. Variations of dc characteristic parameters, such as input offset voltage and input bias current have been studied. Extensive experimental results are presented, including the effects of *annealing*, on critical parameters. It is seen that these devices behave differently on exposure to gamma radiation, depending on the structure of their input stage. The MOSFET-based stages show a greater change in input offset voltage, whereas FET-based input stages exhibit a greater change in input bias currents. Chopper stabilised linear circuits exhibit lesser deviation in their offset voltages and bias currents due to an inherent *chopping action* at their input stage that automatically compensates for any variations in these parameters.**

***Index Terms*—Annealing, gamma radiation, linear circuits, ultra-low input bias current.**

I. Introduction

ULTRA-LOW input bias current (ULIBC) linear circuits (operational amplifiers or op-amps) form an integral part of the input stage of several low current and voltage measurement systems. ULIBC linear circuits have, as the name suggests, typical input bias currents of the order of a few pico Amperes (pA) or sometimes even femto Amperes (fA). On account of these features, they are a natural choice in circuits where the input currents are too small for normal op-amps to handle. Commonly used op-amps have bias currents in the order of a few hundreds of nano ampere (nA) and, thus, would tend to completely *swamp* out the smaller input signals, e.g., the current signals from a pH meter would tend to be in the order of pA or less. If a commonly used op-amp, having a nA range of bias current is used, it would completely *overwhelm* the actual input current signal and the measurement would be totally erroneous. The input impedance of a ULIBC linear circuit is substantially higher than that of normal op-amps and, hence, feeble input signals are much more *faithfully* conditioned (without loading the source). Such is the importance and usefulness of ULIBC devices that a number of companies manufacture these using different technologies. Some of the popular ULIBC devices, the companies manufacturing them and the technology used are given in Table I.

Critical applications of ULIBC linear circuits are space avionics, radiation-monitoring systems, bio-medical systems etc. In space applications, the ULIBC linear circuits play an important role in conditioning the faint signals that might, for example, come from earth or a nearby planet, or while transmitting meteorological data. In radiation monitoring systems, the ULIBC devices may be needed in equipment such as an ion chamber amplifier. As an example of biomedical application, the feeble signals from the heart, brain or eyes may be required to be faithfully conditioned for display in appropriate form—that is to say, the ULIBC linear circuits are used in specially designed systems unlike their common linear circuit counterparts. These special designs require very low leakage printed circuit boards (PCBs) and teflon standoffs for keeping the current leakage to a minimum. The environment (temperature, humidity, pressure, radiation, etc.) in which these devices operate also affects their performance.

Many applications of ULIBC devices require them to work under conditions of nuclear radiation (e.g., gamma radiation). The extent of radiation experienced depends on the specific application. For example, in space applications (where radiation doses are typically around 0.1 to 1 mrad/s), the devices could be subjected to different levels of radiation depending upon whether the mission is low earth orbit (LEO), geo-synchronous earth orbit (GEO), or interplanetary. This causes a breakdown in the devices used in the instrumentation system, resulting in malfunction [1]. In applications related to nuclear installations, the radiation level depends on the proximity of the source and/or prevailing conditions [e.g., is there a leakage or is there loss of coolant accident (LOCA) or is the radiation level normal?]. Irrespective of the application, it is necessary that the behavior of these devices under such conditions be well understood. In fact, one would like to know how the behavior of these devices varies while they are in operation (biased). While a lot of work has been carried out over the last two decades to study the effect of gamma radiation on several electronic devices and integrated circuits (ICs), to the best of our knowledge, no work has been reported so far that exclusively deals with the radiation effects

Manuscript received March 19, 2004; revised July 10, 2004 and October 25, 2004.

The authors are with the Department of Electrical Engineering, Indian Institute of Technology, Bombay, Powai, Mumbai-400 076, India (e-mail: agarwal@ee.iitb.ac.in).

Digital Object Identifier 10.1109/TNS.2005.846872

TABLE I
COMMONLY USED ULIBC LINEAR CIRCUITS

Op-Amp	Company	Type of input stage
DN8500A	Thermoptics	MOSFET
AD549JH	Analog Devices	JFET+
OPA128JM	TI-Burr Brown	DiFET+
LMC6001AIN	National Semiconductor	JFET (?)*
TC7652	Microchip	Chopper stabilised input

+The FET and DiFET stages of Op-Amps AD549JH and OPA128JM differ in the fact that the input stage of the latter is a dielectrically isolated FET stage, as compared to the former.

*This information is not confirmed by National Semiconductor

on ULIBC linear circuits, especially under biased conditions. This paper deals with this aspect.

Indeed, the design and fabrication of ULIBC devices is a challenging task. Their internal circuitry is far more complex and sophisticated as compared to common op-amps. Considering the large market that such devices would attract, it is not surprising that different companies adopt different technologies to realize the desirable features. The important point here is that ULIBC devices of different makes and input stages (e.g., JFET, MOS, etc.) would behave differently on exposure to gamma radiation. It is for this reason that a wide range of devices have been chosen in this work as shown in Table I. The devices chosen for experimentation are DN8500A from Thermoptics, AD549JH from Analog Devices, LMC6001AIN from National Semiconductor, OPA128JM from TI-Burr Brown, and TC7652 from Microchip, primarily on account of their varied input stages.

To summarize, this paper deals with the following.

1) It investigates the effect of gamma radiation on a wide range of ULIBC linear circuits.
2) The study is performed *online*—meaning the circuits are operating (biased) and *in-source* when the measurements are done.
3) Focus is on the small signal dc applications used in nuclear installations. Thus, the important parameters of interest are the input offset voltage (V_{io}) and the input bias current (I_b) of the ULIBC devices.
4) An ambient corresponding to a noncatastrophic radiation leakage is considered for the study. This might occur due to some technical snag. Nuclear reactor environment dose rates are typically around 20 to 40 mrad/h, which might go higher, say 1 to 2 krad/h due to such a noncatastrophic leakage.

The remaining part of this paper is divided into the following sections. Section II carries a brief overview of the research work done so far on linear circuits in general. Section III presents procedural details of the experimental study on *biased* ULIBC devices *in-source*. Observation and discussion of results are presented in Section IV, while major conclusions of this work are summarized in Section V.

II. Literature Review

A lot of research has transpired in the area of gamma radiation effects on both discrete semiconductor devices as well as linear circuits. While the research on the radiation effects on discrete devices started in the sixties, linear circuits became the focus of study during the last couple of decades [2]–[20]. This is not to say that the former are not considered any more, since the discrete devices, indeed, are the *building blocks* of any linear circuit. There is still a good amount of research carried out to understand the radiation effects on MOS devices with an equal emphasis on *hardening* MOS-systems against radiation damage [21], [22]. These efforts, in turn, serve as a base for studying those linear circuits that have, say, a MOS-based input stage. For example, N_{OT} and N_{IT} play an important role in deciding the nature of the MOS characteristics [23] and radiation affects these traps.

The issues addressed in the radiation effects research on linear circuits are manifold. One of them is the radiation behavior of linear circuits depending upon the type of input stage, i.e., bipolar, FET or MOS-based. Linear bipolar devices, particularly those with *pnp* stages show a significant degradation at dose rates lower than 10 mrad(Si)/s [2]–[4]. It has been shown that *pnp* and *substrate-pnp (spnp)* input structures have been observed to deteriorate more than those with *npn* super-structures and are much less damaged for the same radiation levels [5]. Linear devices having *lateral-pnp(lpnp)* input structures degrade significantly than those having *spnp* input structures [6]. True dose rate effects (TDREs) are particularly prevalent in bipolar technologies, while time dependent effects (TDEs) are well-known effects in CMOS technologies [10]. FET-based linear circuits could show a radiation behavior depending upon the change in the reverse saturation currents across the diode junction at the input.

Another important issue that has been actively pursued over the years is the effect of total dose and dose rate effects on linear circuits. The issue of total dose variation in linear bipolar op-amps and comparators has been addressed in [7], where *pre-irradiation bakes* of these linear devices have been shown to affect total-dose degradations in comparators and LM124 op-amps, due to the build-up of N_{OT} and N_{IT}. For a given total dose, changes in the critical parameters of linear devices are found to be highly nonlinear and hence are erratic functions of the dose rate [8].

As far as dose rate issues are concerned, the main distinguishing feature between linear devices that are low-dose-rate sensitive and those that are not sensitive manifests itself in the form of differences in the structure of the oxide growth on these devices. The former has sharper transition levels between the thin and thick oxides when compared to the gentle transition in the latter, resulting in reduced hydrogen bonds or difference in

TABLE II
CHARACTERISTICS OF THE ULIBC OP-AMPS USED IN THE STUDY

Device	Z_{in}	Max. I_b	Max. V_{io}	CMRR
DN8500A	$10^{13}\Omega$	0.01 pA	50 mV	75 dB
AD549JH	$10^{13}\Omega$	0.25 pA	0.5 mV	90 dB
OPA128JM	$10^{12}\Omega$	0.30 pA	1 mV	118 dB
LMC6001AIN	$10^{12}\Omega$	0.025 pA	0.3 mV	75 dB
TC7652	$10^{12}\Omega$	30 pA	5 μV	140 dB

Z_{in} – Input impedance I_b – Input bias current V_{io} – Input offset voltage

oxide density or strain [5]. Bonora *et al.* [9] reiterate the findings that linear bipolar ICs undergo more damage at lower dose rates (around 3 mrad(Si)/s) and also bring out the importance of biasing conditions on the ICs during irradiation at elevated temperature. Both TDRE (esp. for bipolar technologies) and TDE (especially for CMOS technologies), have to be considered while characterising low dose-rate effects [10].

Another aspect is that of accelerated testing, which is more suitable for MOS-based linear devices than bipolar ones since the latter fail at much lower dose rates then the former [11]. Accelerated total dose testing, i.e., experiments done at high dose rate and high temperature are shown to closely determine tolerance at very low dose rate and at room temperature (RT) [12]. Also, this is shown to be more valid for determining bias parameter degradation than offset parameters at low dose rate, at RT.

An important issue addressed is that of geometry in linear bipolar circuits [13], [14] which plays an important role in the degradation of linear devices due to radiation that could be either electron or gamma energy. Yet another aspect that affects the magnitude of degradation due to irradiation is the history of previous irradiation done on the linear devices [10], [11]. Noise performance is also a vital parameter that has been studied for radiation effects, particularly in precision bipolar linear circuits. Both voltage and current noise degrade significantly, at high- and low-dose rates, respectively [15], [16].

Radiation hardness is also an important issue that has been extensively dealt with, where device degradation (due to radiation) issues are taken into consideration while designing commercially available off the shelf (COTS) devices [17]. For improving total ionising dose (TID) hardness in these devices, *guarding* could be provided to avoid radiation induced parasitic leakage or reduced usage of hydrogen during wafer processing. Single event transients (SETs) issues may be handled using high value feedback resistors, switched capacitors and cross coupled transistors, while latch up and transient dose rate immunity problems may be overcome by use of epitaxial substrates [17].

One of the major endeavours in this field of research has been to device schemes that would ensure the *hardness* of these devices against irradiation. This issue has been addressed by Pease *et al.* [18], where a hardness test method is proposed to identify the linear devices exhibiting enhanced low dose rate sensitivity (ELDRS). This has been evaluated to arrive at an optimal dose rate of 10 mrad(Si)/s at RT or elevated dose rate at 100°C. Also, parameters such as *design margins* have been defined [19] that help in *estimating* the low dose rate at RT by high dose rate accelerated tests at around 100°C. A practical result of ELDRS of linear circuits in space applications has been demonstrated by Titus *et al.* [20], where hardness assurance tests were applied to predict ELDRS, with appropriate design margins.

In the entire gamut of literature available, it was concluded that there is not much literature available on the ULIBC op-amps that are vital for nuclear and analytical instrumentation. Hence, it was felt that an experimental study done on the radiation effects on ULIBC op-amps, would help in better understanding of the dc small signal parametric changes of these devices and hence, in general, the instrumentation associated with them, under irradiation. This is necessary, since bias and offset parameters are the most critical parameters that degrade with ionising radiation. Also, given the specialised critical applications in which ULIBC linear devices are used, it is important that their radiation profile be characterized to prevent "system upsets."

III. DEVICE TYPES AND EXPERIMENTATION

A two-pronged approach was followed in the research reported in this paper. One was with respect to the choice of devices themselves, i.e. all of them were ULIBC op-amps. Secondly, each of them was from a different manufacturer and their input structures were different. The idea of doing this was to compare the behavior of the ULIBC op-amps *vis-à-vis* their *online* radiation profile for similar total doses and dose rates. The dose rate chosen for the experimental work was 2.79 krad(Si)/h or 0.77 rad(Si)/s obtained from a Co-60 source.

A. Characteristics of the ULIBC Linear Devices Chosen for Experimentation

The input stages of the ULIBC devices could be MOS-, JFET-, or CMOS-based. The MOS-based input stages have the advantage of having very low I_b due to an inherent insulation between the gate and the source/drain. However, their offset voltages are much higher than JFET and CMOS input stage devices. The JFET-based input stage devices have the advantage of withstanding higher electro-static discharge (ESD) since their input stage is a diode junction. However, due to this, they do not fare well with temperature variations. The CMOS-based input stages are known to have inherent low power consumption and have good temperature dependence. The characteristics of all the devices chosen for the radiation experiments are summarized in Table II.

B. Experimental Setup and Procedure

Each of the ULIBC linear devices was tested for its nascent characteristics by using it in a circuit shown in Fig. 1. The sim-

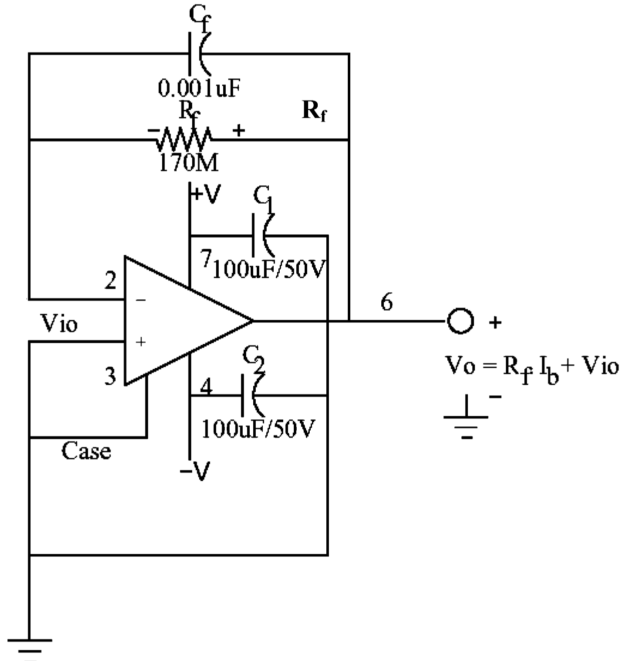

Fig. 1. Circuit schematic used to measure nascent characteristics of ULIBC linear devices.

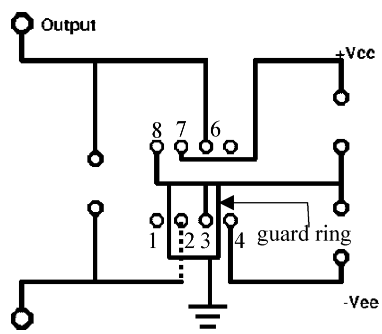

Fig. 2. PCB layout of the scheme used in measurement of nascent characteristics of ULIBC linear devices having DIP plastic package.

ulation of the above circuit was carried out using SABER software. The output voltage is a function of both I_b and V_{io}. The V_{io} is found by shorting the resistor R_f. The I_b is found out by the following equation:

$$I_b = \frac{V_o - V_{io}}{R_f}. \tag{1}$$

It was ensured that the output did not saturate because the output of op-amp was able to swing ± 13 V when appropriate input signals were given. Figs. 2 and 3 show the PCB layouts of the ULIBC devices for the experimental setup for the DIP and TO-99 metal can packages, respectively. The *guard rings* are necessary for the ULIBC devices to avoid even the fA leakage that may deteriorate their performance [24]. The PCBs were designed to achieve ultra-low leakage by islanding and use of teflon standoffs as shown in Fig. 4. The *guard-ring* terminals on the PCB were grounded so as to sweep out any leakages. The noninverting terminal too, was grounded, as shown in Figs. 2 and 3. The value of R_f used was 330 $\mathrm{M}\Omega$ for OPA128JM and TC7652, 680 $\mathrm{M}\Omega$ for LMC6001AIN and AD549JH, and 4.7 GΩ for DN8500A. The measurements on all devices were recorded at equal and frequent intervals of time. Once an irradiation of about 15 krad(Si) was reached, an *annealing* time of approximately 15 h was allowed for each sample of the ULIBC op-amps before resuming irradiation. After annealing, the samples were again irradiated upto a cumulative dose of $\approx$39 krad(Si). The pre and post-irradiation V_{io} values are reproduced in Tables III and IV, respectively, while the pre-intermediate and post irradiation values of I_b are tabulated in Table V.

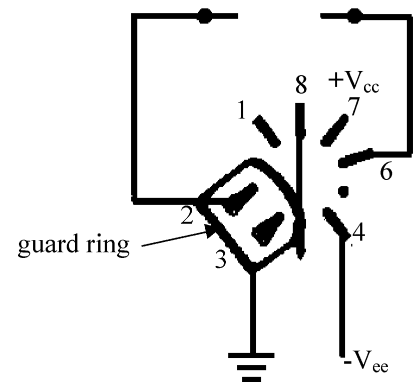

Fig. 3. PCB layout of the scheme used in measurement of nascent characteristics of ULIBC linear devices having TO-99 metal can package.

IV. Observation and Discussion of Results

A. *Performance of DN8500A*

Figs. 5 and 6 show the effect of radiation at a dose rate of 0.77 rad(Si)/s on the V_{io} and I_b, respectively, of DN8500A. The DN8500A has an n-channel MOSFET input stage because of which there is a larger change in its V_{io} due to radiation as compared to the change in its I_b value. Since the applied bias drives out most of the electrons from the oxide insulator, the holes, having lesser mobility than the electrons, get trapped in the SiO_2-gate interface (for positive gate voltages) and in the SiO_2-gate metal interface (for negative gate voltages) [22]. This trapping is one of the primary reasons for the change in the V_{io} of the device.

Since all the experiments and the corresponding observations are carried out when the circuit is *biased* and the radiation is *on*, radiation-induced photocurrents play an important role in the behavior of the vital parameters of the ULIBC devices, i.e., V_{io} and I_b. As seen in Figs. 5 and 6, both V_{io} and I_b show a "drop" in their values as soon as the irradiation is turned *off* after the first 15 krad(Si), thereby highlighting the effect of induced photo currents. This is shown by segments P-Q and $P' - Q'$ respectively, which join the points just before and after the first 15 krad(Si).

The V_{io} jump (when the source is turned *off*) could be due to the fact that the radiation-induced photo currents are not equal in the two devices of the input differential stage. If the radiation-induced photo currents are equal in the two devices, they become *common-mode* currents, and would have a limited effect on V_{io}. It may be noted that the photo currents cause the curves to be nonmonotonic in nature. It is also seen that V_{io} increases gradually with an increase in the irradiation. Further, as

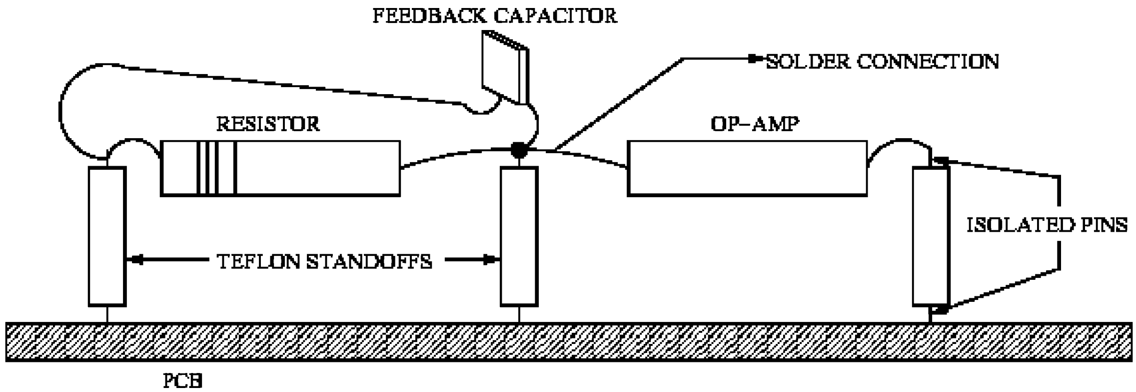

Fig. 4. Quality PCB design for ULIBC linear devices using Teflon standoffs, where *air-wiring* is used (input pins of the ULIBC op-amp are lifted out of the PCB and soldered onto the Teflon standoffs, so that there is an inherent isolation between the pins and the PCB).

TABLE III
PREIRRADIATION V_{io} VALUES OF THE ULIBC OP-AMPS CONSIDERED

DN8500A (mV)			AD549JH (mV)			OPA128JM (mV)			LM6001AIN (mV)		TC7652 (μV)		
S1	S2	S3	S1	S2	S3	S1	S2	S3	S1	S2	S1	S2	S3
2.41	2.45	2.0	0.15	0.14	0.19	0.01	0.14	0.10	0.32	0.54	5.6	5.4	6.0

TABLE IV
POSTIRRADIATION V_{io} VALUES OF THE ULIBC OP-AMPS CONSIDERED

DN8500A (mV)			AD549JH (mV)			OPA128JM (mV)			LM6001AIN (mV)		TC7652 (μV)		
S1	S2	S3	S1	S2	S3	S1	S2	S3	S1	S2	S1	S2	S3
1.93	1.25	1.53	2.32	2.40	2.54	1.01	0.62	0.81	2.09	1.4	6.1	5.8	7.4

TABLE V
PRE- AND POSTRADIATION VALUES OF THE INPUT BIAS CURRENT

	DN8500A			AD549JH			OPA128JM			LM6001AIN		TC7652		
	S1	S2	S3	S1	S2	S3	S1	S2	S3	S1	S2	S1	S2	S3
(a)	0.05	0.06	0.05	1.36	1.29	1.10	1.43	1.57	1.45	0.10	0.14	80	85	73
(b)	0.15	0.14	0.15	0.26	0.19	0.22	1.43	3.17	3.09	0.32	0.37	0.13	0.19	0.23
(c)	0.13	0.14	0.16	0.21	0.12	0.15	1.05	3.20	3.15	0.31	0.33	0.16	0.26	0.31

(a) : Pre-radiation values of I_b (pA)
(b) : Post-radiation values of I_b (nA) immediately after the source is turned off for the intermediate annealing period
(c) : Final Post-radiation values of I_b (nA)

soon as the radiation is turned off, it is seen that their magnitudes take a drastic dip and do not go back to their initial values (just before radiation was turned off). This effect could be due to annealing. In the case of I_b, the deviation is lesser as compared to V_{io} during the *anneal* period. The increase in I_b may be due to increase in the surface leakage due to irradiation. On completion of the total dose of 39 krad(Si), the irradiation was stopped, and it was found that the V_{io} and I_b values had decreased.

B. Performance of AD549JH

The AD549JH has a JFET input stage resulting in a low I_b. Since the input is inherently a diode junction, the main cause of change in I_b would be due to the increase in the radiation-induced photo current across this junction. This is seen in Fig. 8, where, with the turning *off* of the radiation source, the I_b falls drastically. The V_{io} is inherently stable in JFET input op-amps, since the radiation-induced photo currents in the channel are small and nearly equal in both the devices at the input stage, as shown in Fig. 7. The *annealing* effect is more pronounced in the case of I_b than that of V_{io}. In Fig. 8, segment $R' - S'$ corresponds to the *anneal* region.

C. Performance of OPA128JM

The OPA128JM has a DiFET input stage which is a FET stage similar to the AD549JH, with dielectric isolation. Figs. 9 and 10 show the V_{io} and I_b irradiation profiles of the op-amp. It is seen that the relative change in V_{io} is much less than that of I_b. Since this is also a JFET device, it behaves similar to AD549JH. The lesser change in I_b, as compared to AD549JH, may be due to

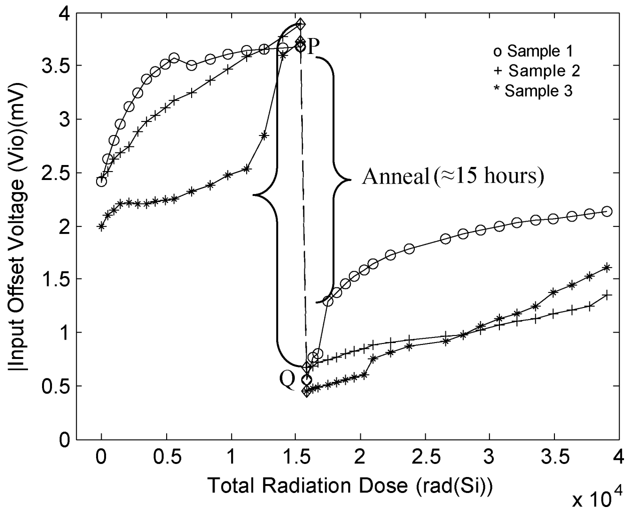

Fig. 5. Variation of V_{io} of DN8500A, as a function of total irradiation dose.

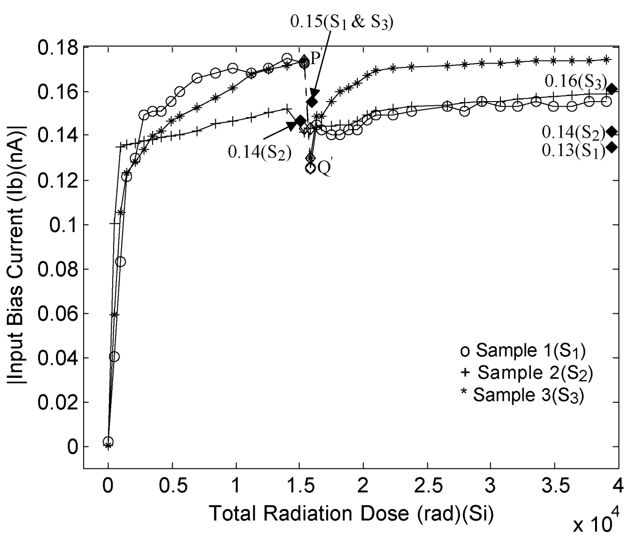

Fig. 6. Variation of I_b of DN8500A, as a function of total irradiation dose.

the dielectric isolation of the op-amp, as shown in the region marked by $L' - M'$ in Fig. 10.

D. Performance of LMC6001AIN

The V_{io} of the op-amp shows an almost continuous change over the period of irradiation and shows no *annealing* effect, as shown in Fig. 11. The I_b shows a jump once the irradiation is turned *off*, as shown by the segment $A' - B'$ in Fig. 12. This behavior is similar to the one observed for a JFET input op-amp, the AD549JH and, hence, would suggest a JFET input structure. Efforts to obtain information about the input stage of LMC6001AIN from National Semiconductors were not successful, since this is a proprietary issue.

E. Performance of TC7652

The TC7652 is a chopper stabilised op-amp that has a different input structure than the rest considered above. The chopping action converts the dc input to ac and is followed by an ac amplifier, as shown in Fig. 13. Hence, the effect of V_{io} and

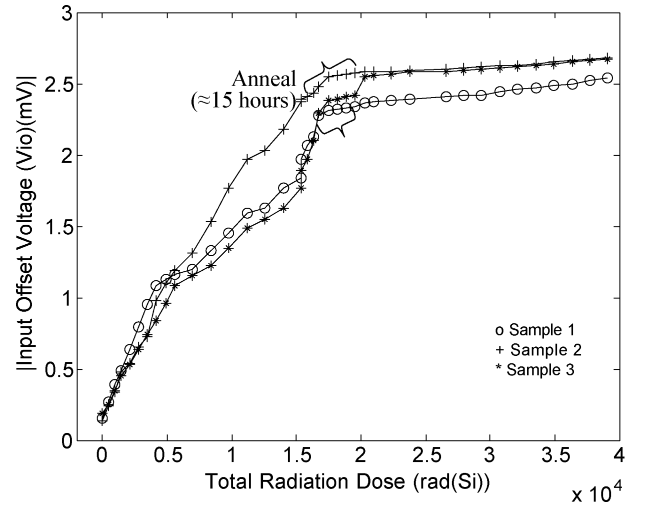

Fig. 7. Variation of V_{io} of AD549JH, as a function of total irradiation dose.

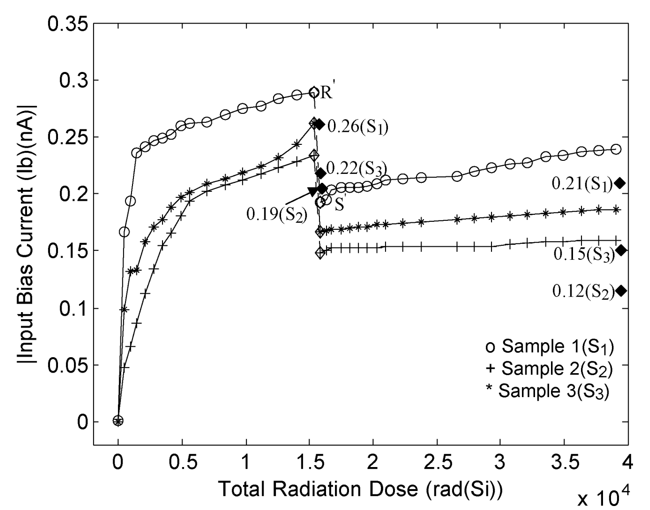

Fig. 8. Variation of I_b of AD549JH, as a function of total irradiation dose.

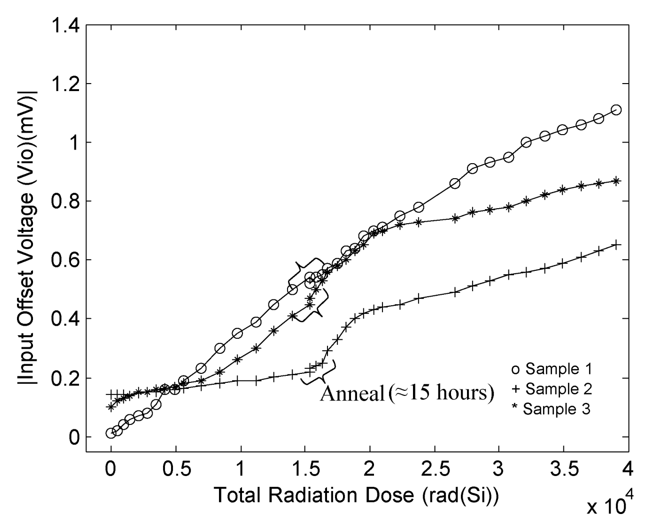

Fig. 9. Variation of V_{io} of OPA128JM, as a function of total irradiation dose.

I_b on the output is negligible. The internal structure of such devices essentially consists of switches, oscillators, amplifiers, etc., along with the main amplifier.

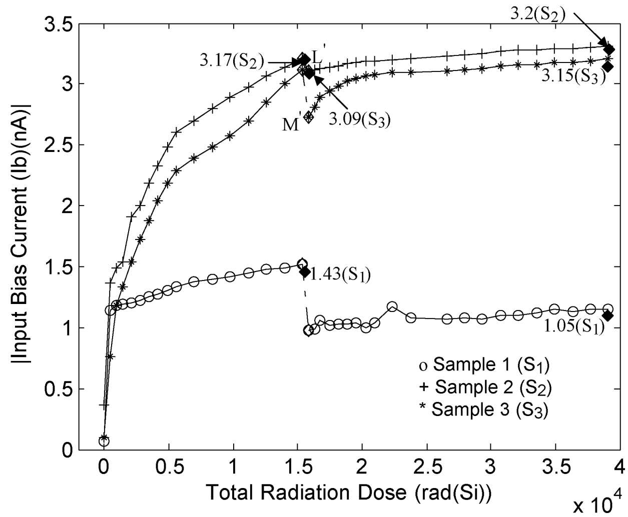

Fig. 10. Variation of I_b of OPA128JM, as a function of total irradiation dose.

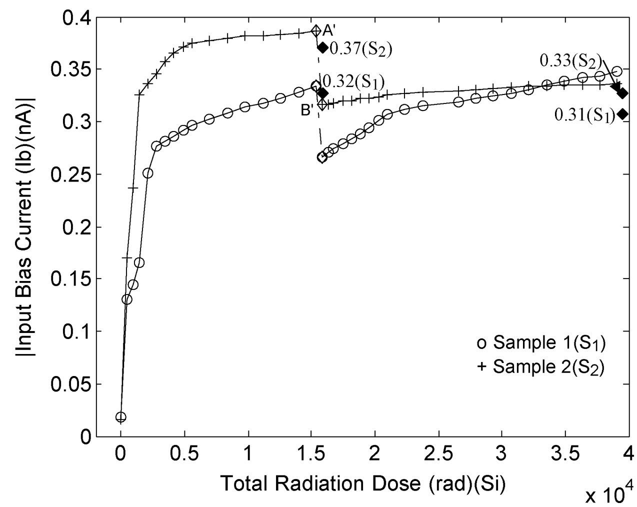

Fig. 12. Variation of I_b of LMC6001AIN, as a function of total irradiation dose.

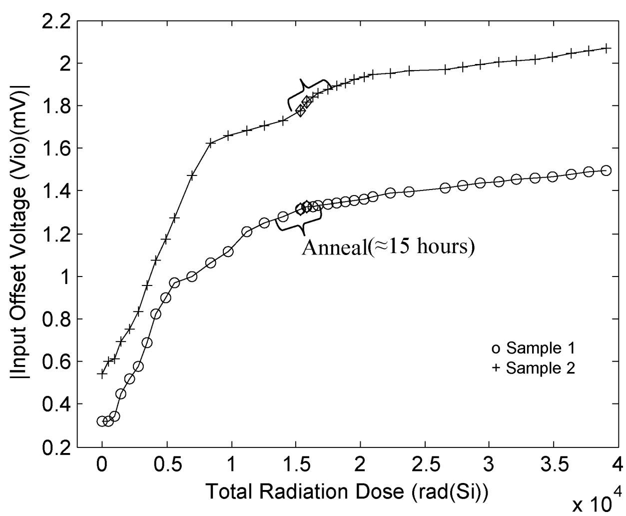

Fig. 11. Variation of V_{io} of LMC6001AIN, as a function of total irradiation dose.

As shown in Fig. 13, S_1 and S_2 are MOS switches, typically switched at a high frequency (~100 kHz). The input is the dc voltage to be amplified. The switching action of S_1 converts it into an ac voltage, which is amplified by an ac amplifier of gain G.

The output of the amplifier is an ac, coupled to an integrator whose time constant (given by R_1C_1) is much larger than the switching frequency. Since S_2 is also switched at the same frequency and phase as that of S_1, V_o is an amplified dc voltage. $V_o \times (R_2/(R_1+R_2))$ is the voltage fed back to the input. At equilibrium, $V_o \times (R_2/(R_1+R_2)) = V_{in}$, so that the average voltage across the capacitor C due to the input voltage V_{in} is zero.

Figs. 14 and 15 show the irradiation trends of V_{io} and I_b, respectively. It is seen that there is continuous deviation of both V_{io} as well as I_b over the period of irradiation. The percentage change in V_{io} and I_b is much lesser than all the other devices considered above, due to automatic internal compensation. Hence, such a device would be more useful in an electronic system that is required to operate in a radiation environment.

V. Conclusion

This paper has presented a comparative study of the irradiation effects on *biased* ULIBC op-amps that have different input stages, with the findings as summarized as follows.

1) The generation of the radiation-induced photo currents plays an important role in the performance of ULIBC devices under *biased*, *in-source* conditions.
2) Due to the photo current generation phenomenon, the curves tend to be nonmonotonic. It must be noted, however, that the ideal condition is to achieve balance. However, in practice, we do not have balance and that is why we can not operate the op-amp in open loop. There are always area, base width and channel length tolerances for the differential stage. In addition, defect density in the two device volumes need not be same. Hence, different photocurrents may be observed in a differential pair.
3) The variation in V_{io} is caused due to several factors and it is not possible to separate these effects. It is quite possible, for example, that surface effects might be saturating beyond a certain radiation dose resulting in a slower or negligible variation in V_{io}. The variation in bias current, on the other hand, is not only due to the generated photo current, but may also be due to surface leakage (packaging) effects from the passivation material. It is difficult to separate these effects.
4) For MOSFET input devices, both V_{io} and I_b show *annealing* effects. The effect is more pronounced in the case of V_{io} than I_b. This could be due to the fact that the radiation-induced photo currents are not equal in the two devices of the input differential stage, thereby dominating the V_{io} change, where as surface leakage currents increase only slightly due to irradiation, thereby not causing a large change in the I_b value.
5) For FET (JFET or DiFET) devices, the V_{io} does not exhibit annealing effects while the I_b does. This is again a result of radiation-induced photo currents, which are more predominant since the phenomenon of trapped

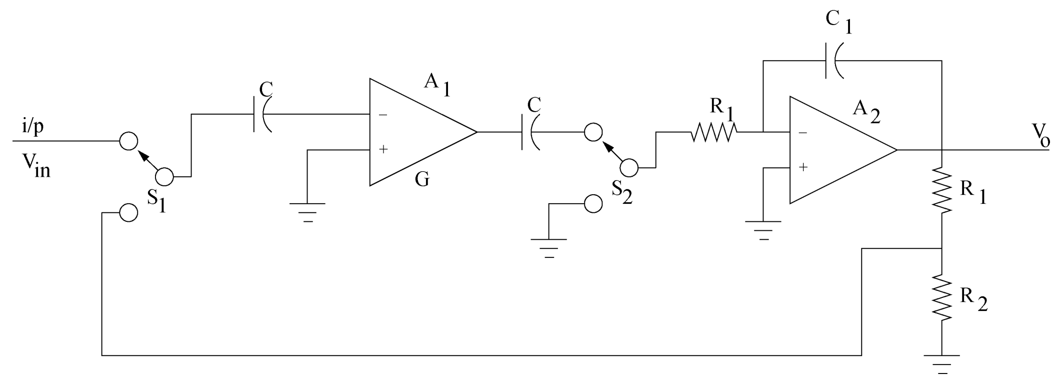

Fig. 13. Internal circuit diagram of a chopper-stabilized configuration in an op-amp.

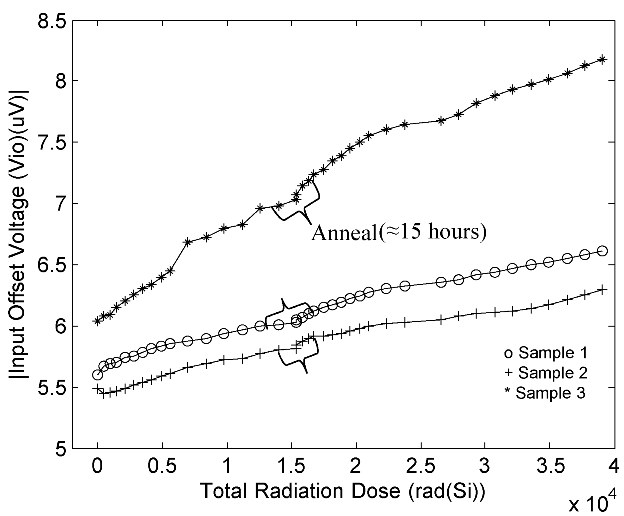

Fig. 14. Variation of V_{io} of TC7652, as a function of total irradiation dose.

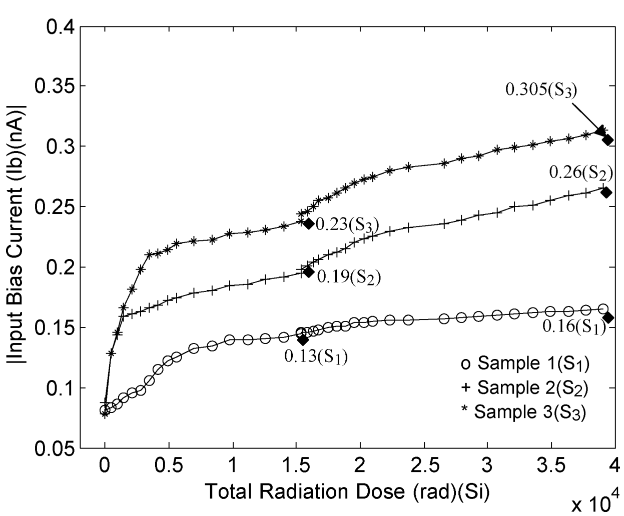

Fig. 15. Variation of I_b of TC7652, as a function of total irradiation dose.

charges does not play a significant role in such devices. The V_{io} does not show much change in these devices, since the radiation-induced photo currents in the channel are small and nearly equal in both the devices at the input stage. The I_b, on the other hand, shows significant change, since radiation-induced photo currents increase across the diode junction in these devices.

6) It is concluded that the LMC6001AIN is a ULIBC device that has a FET input stage, since the recorded observations show its parametric behavior to be quite similar to that of the AD49JH and OPA128JM which are JFET and DiFET input devices, respectively.

7) Chopper stabilised amplifiers, such as the ULIBC device TC7652 analyzed in this paper, show very less parametric changes under biased, irradiated conditions. This is due to the conversion of input dc to ac by the *chopping* action, resulting in automatic compensation for changes in V_{io} and I_b. If a MOSFET is used as a switch, as in the case of a chopper stabilised amplifier, then V_{io} and I_b variation have less effect on the performance than when it is used in a linear application. Similarly, if the JFET is used as a switch in a chopper stabilised amplifier, the I_b degradation doesn't affect the chopping action. Thus, if chopper stabilised op-amps are used for low current applications, their performance will be much superior under radiation environment.

The main impact in any critical application, owing to the changes in the V_{io} and I_b of the ULIBC linear device, would be lowering of its "sensitivity" to detect the weakest of input signals, thereby rendering the detection and signal conditioning system of the ULIBC linear device ineffective. The limit on I_b will be governed by the application. In applications, such as an ion chamber amplifier, the sensed current is very weak and hence the first stage of the amplifier and conditioning circuit is invariably a unity gain buffer. The I_b should be at least one order lower than the current to be sensed. Considering that the leakage radiation around it may rise up to 1–2 krad(Si)/h or higher, the change in ULIBC linear circuit parameters (V_{io} and I_b) would directly affect, for example, the low current limit of a current measuring I-V converter. If I_b is critical, one needs to minimize the collection volume by using some form of silicon-on-insulator (SOI) like silicon-on-sapphire (SOS), bonded wafer or separation by implantation of oxygen (SIMOX). However, if bias current requirements are not extremely critical and the input signal is of differential input type, then the TC7652 would be a better solution.

REFERENCES

[1] A. R. Frederickson, J. M. Ratliff, and G. M. Swift, "On-orbit measurement of JFET leakage current and its annealing as functions of dose and bias at Jupiter," *IEEE Trans. Nucl. Sci.*, vol. 49, no. 6, pp. 2759–2764, Dec 2002.

[2] A. H. Johnston, G. M. Swift, and B. G. Rax, "Total dose effects in conventional bipolar transistors and linear integrated circuits," *IEEE Trans. Nucl. Sci.*, vol. 41, no. 6, pp. 2427–2436, Dec. 1994.

[3] S. McClure, R. L. Pease, W. Will, and G. Perry, "Dependence of total dose response of bipolar linear microcircuits on applied dose rate," *IEEE Trans. Nucl. Sci.*, vol. 41, no. 6, pp. 2544–2549, Dec. 1994.

[4] J. Beaucour, T. Carriere, and A. Gach, "Total dose effects on negative voltage regulator," *IEEE Trans. Nucl. Sci.*, vol. 41, no. 6, pp. 2420–2426, Dec. 1994.

[5] A. H. Johnston, C. I. Lee, and B. G. Rax, "Enhanced damage in bipolar devices at low dose rates: effects at very low dose rates," *IEEE Trans. Nucl. Sci.*, vol. 43, no. 6, pp. 3049–3059, Dec. 1996.

[6] D. M. Schmidt, A. Wu, R. D. Schrimpf, D. M. Fleetwood, and R. L. Pease, "Modeling ionizing radiation induced gain degradation of the lateral PNP bipolar junction transistor," *IEEE Trans. Nucl. Sci.*, vol. 43, no. 6, pp. 3032–3039, Dec. 1996.

[7] H. J. Barnaby, C. R. Cirba, R. D. Schrimpf, D. M. Fleetwood, R. L. Pease, M. R. Shaneyfelt, T. Turflinger, J. F. Krieg, and M. C. Maher, "Origins of total-dose response variability in linear bipolar microcircuits," *IEEE Trans. Nucl. Sci.*, vol. 47, no. 6, pp. 2342–2349, Dec. 2000.

[8] A. H. Johnston, B. G. Rax, and C. I. Lee, "Enhanced damage in linear bipolar integrated circuits at low dose rate," *IEEE Trans. Nucl. Sci.*, vol. 42, no. 6, pp. 1650–1659, Dec. 1995.

[9] L. Bonora and J. P. David, "An attempt to define conservative conditions for total dose evaluation in linear bipolar ICs," *IEEE Trans. Nucl. Sci.*, vol. 44, no. 6, pp. 1974–1980, Dec. 1997.

[10] R. K. Freitag and D. B. Brown, "Low dose rate effects on linear bipolar ICs: Experiments on the time dependence," *IEEE Trans. Nucl. Sci.*, vol. 44, no. 6, pp. 1906–1913, Dec. 1997.

[11] ——, "Study of low-dose-rate radiation effects on commercial linear bipolar ICs," *IEEE Trans. Nucl. Sci.*, vol. 45, no. 6, pp. 2649–2658, Dec. 1998.

[12] T. Carriere, R. Ecoffet, and P. Poirot, "Evaluation of accelerated total dose testing of linear bipolar circuits," *IEEE Trans. Nucl. Sci.*, vol. 47, no. 6, pp. 2350–2357, Dec. 2000.

[13] A. H. Johnston and R. E. Plaag, "Models for total dose degradation of linear integrated circuits," *IEEE Trans. Nucl. Sci.*, vol. NS-34, no. 6, pp. 1474–1480, Dec. 1987.

[14] B. G. Rax, A. H. Johnston, and T. Miyahira, "Displacement damage in bipolar linear integrated circuits," *IEEE Trans. Nucl. Sci.*, vol. 46, no. 4, pp. 1660–1665, Aug. 1998.

[15] D. M. Hiemstra, "Dose rate dependence of the current noise performance of an ultra-low noise precision bipolar operational amplifier," *IEEE Trans. Nucl. Sci.*, vol. 46, no. 6, pp. 1674–1679, Dec. 1999.

[16] ——, "Total dose performance of a commercial off the shelf ultra-low noise precision operational amplifier during irradiation," in *Proc. IEEE Radiation Effects Data Workshop Record*, July 1997, pp. 80–83.

[17] P. S. Winokur *et al.*, "Use of COTS microelectronics in radiation environments," *IEEE Trans. Nucl. Sci.*, vol. 46, no. 6, pp. 1494–1503, Dec. 1999.

[18] R. L. Pease, L. M. Cohn, D. M. Fleetwood, M. A. Gehlhausen, T. L. Turflinger, D. B. Brown, and A. H. Johnston, "A proposed hardness assurance test methodology for bipolar linear circuits and devices in a spring ionising radiation environment," *IEEE Trans. Nucl. Sci.*, vol. 45, no. 6, pp. 2665–2672, Dec. 1998.

[19] R. L. Pease, M. Gehlhausen, J. Krieg, J. Titus, T. Turflinger, D. Emily, and L. Cohn, "Evaluation of proposed hardness assurance method for bipolar linear circuits with enhanced low dose rate sensitivity (ELDRS)," *IEEE Trans. on Nucl. Sci.*, vol. 45, no. 6, pp. 2665–2672, Dec. 1998.

[20] J. L. Titus, D. Emily, J. F. Krieg, T. Turflinger, R. L. Pease, and A. Campbell, "Enhanced low dose rate sensitivity (ELDRS) of linear circuits in a space environment," *IEEE Trans. Nucl. Sci.*, vol. 46, no. 6, pp. 1608–1619, Dec. 1999.

[21] G. C. Messsenger and M. S. Ash, *Effects of Radiation on Electronic Systems*. New York: Van Nostrand Reinhold, 1986.

[22] T. P. Ma and P. V. Dressendorfer, *Ionising Radiation Effects on MOS Devices and Circuits*. New York: Wiley, 1989.

[23] V. P. Sundarsingh and R. P. Das, "Study of the origin of double peaks in the capacitance voltage plots of $\mathrm{Al} - \mathrm{SiO_2} - \mathrm{Si}$ capacitors," *Int. J. Electron.*, vol. 57, no. 4, pp. 535–541, 1984.

[24] National Semiconductor Databook, National Semiconductor.